Reactions on Atmospheric Dust Particles: Surface Photochemistry and Size-Dependent Nanoscale Redox Chemistry

ARTICLE *in* JOURNAL OF PHYSICAL CHEMISTRY LETTERS · JUNE 2010

Impact Factor: 7.46 · DOI: 10.1021/jz100371d

THE JOURNAL OF PHYSICAL CHEMISTRY Letters

PERSPECTIVE

pubs.acs.org/JPCL

Reactions on Atmospheric Dust Particles: Surface Photochemistry and Size-Dependent Nanoscale Redox Chemistry

Gayan Rubasinghege,[†] Sherrie Elzey,[‡] Jonas Baltrusaitis,[†] Pradeep M. Jayaweera,[†] and Vicki H. Grassian*[,†,‡]

[†]Department of Chemistry and [‡]Department of Chemical and Biochemical Engineering, University of Iowa, Iowa City, Iowa 52242

ABSTRACT Mineral dust aerosol is indisputably an important component of the Earth's atmosphere and provides a reactive surface for heterogeneous chemistry to occur. These reactions can alter concentrations of key trace atmospheric gases as well as change the physicochemical properties of the dust particles. The focus of this Perspective article is on several new mechanisms and reaction pathways identified in laboratory studies on components of mineral dust and on nanodust, a potentially new source of metal-containing dust from engineered nanomaterials. These reactions include surface photochemical mechanisms for renoxification and sulfur dioxide oxidation and size-dependent redox chemistry of metal-containing dusts in low-pH environments including naturally occurring iron oxides and engineered metal nanoparticles. These newly identified reactions have the potential to play an important role in atmospheric chemistry.

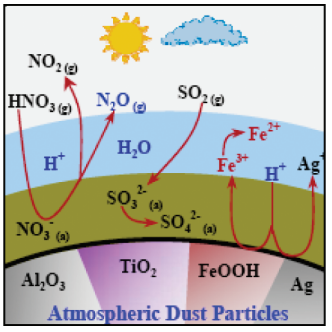

Mineral dust is a reactive component of the tropospheric aerosol.[1,2] It is now widely recognized that reactions on mineral dust aerosol impact both the chemical balance of the atmosphere and the physicochemical properties of the particles, which, in turn, can change the climate impact of these particles (i.e., light scattering efficiency and cloud and ice nucleation activity). Field studies using single-particle analysis have now shown that the chemistry is mineralogy-specific and follows the trends expected and predicted from laboratory studies.[3−7]

What is the role of heterogeneous photochemistry in the troposphere and how does the day time chemistry of mineral dust aerosol differ from night time chemistry?

In this Perspective, we focus on several new classes of reactions on atmospheric dusts that have recently been identified in laboratory studies. These reactions include surface photochemistry and nanoscale size-dependent redox chemistry on components of mineral dust and nanodust, that is, dust produced from engineered nanomaterials or other industrial sources, that can potentially play an important role in atmospheric chemistry. Given that there is increasing evidence for anthropogenic sources of metal-containing dusts in the atmosphere,[8,9] nanodusts, many of which are metal-based nanomaterials, may be a source of soluble metals following heterogeneous and multiphase reactions in the atmosphere.[10]

Figure 1 shows a cartoon drawing of the life cycle of atmospheric dusts in terms of emission, transport, and deposition into aqueous and terrestrial ecosystems as a modified "aged" dust particle. The focus here is on the important yet sometimes poorly understood physical and chemical processes that can take place on the particle surface during atmospheric transport (including interfacial and heterogeneous chemistry, multiphase chemistry, cloud processing, and surface photochemistry). The presence of the sun in Figure 1 should be noted as, in many ways, laboratory studies on the heterogeneous chemistry of mineral dust aerosol in the past 10 years have focused mainly on the night time chemistry of dust.[2] This focus can in some ways be regarded as being representative of only half of the problem. Given that photochemistry dominates the day time gas-phase chemistry of the atmosphere and new light-induced pathways continue to be discovered,[11] along with the realization that the surface and near-surface regions of particles catalyze and promote reactions that perturb the composition of the troposphere, one can ask, what is the role of heterogeneous photochemistry in the troposphere and how does the day time chemistry of mineral dust aerosol differ from night time chemistry? Although these solar-initiated reactions may be of significance in the atmosphere, there is still much to be learned about photochemical reactions involving mineral dust aerosol.

Received Date: March 20, 2010
Accepted Date: May 7, 2010
Published on Web Date: May 17, 2010

DOI: 10.1021/jz100371d | J. Phys. Chem. Lett. 2010, 1, 1729–1737

THE JOURNAL OF PHYSICAL CHEMISTRY Letters

PERSPECTIVE

pubs.acs.org/JPCL

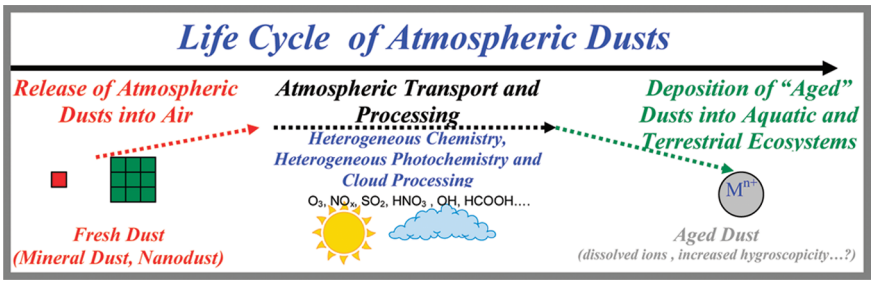

Figure 1. Cartoon representation of the life cycle of atmospheric dusts. These dust particles are emitted into the atmosphere and then undergo long-range transport, with important yet, in some cases, poorly understood chemical and physical processes including heterogeneous chemistry with trace gases, photochemistry, cloud chemistry, and so forth. These "aged" dust particles then undergo deposition into aqueous and terrestrial ecosystems with very different physicochemical properties from the freshly emitted dust particles.

Here, we present several surface photochemical mechanisms identified in laboratory studies. The first mechanism involves the 310 nm photolysis of nitrate adsorbed on aluminum oxide particles, proxies for dust aerosol, to yield gas-phase nitrogen oxides. This reaction is potentially significant as it defines a route for the renoxification of the atmosphere whereby nitric acid, usually considered a reservoir species that, once associated with particulate matter such as dust, is removed from the atmosphere now becomes a source of NO_x (NO_x = NO + NO_2). The second photochemical pathway investigated is the oxidation of SO_2. In particular, the photochemical oxidation of sulfur dioxide on the surface of titanium dioxide particles is discussed. Titanium dioxide is a light-absorbing, photocatalytic component of mineral dust and, as discussed in this article, readily oxidizes adsorbed sulfite to sulfate. The oxidation of sulfur dioxide to sulfate on mineral dust is a poorly understood process,[9,10] and there may be several mechanisms operative, including the surface photochemical one involving an adsorbed sulfite intermediate, as discussed here.

Redox reactions involving mineral dust are also of great interest, especially for iron-containing minerals, as iron from iron-containing mineral dust, transported and deposited into certain regions of the ocean, is often a limiting nutrient for ocean life.[14] It has been proposed that reactions of mineral dust with trace atmospheric gases such as HNO_3 lead to very low pH environments, as low as pH 1 or 2.[15] Partitioning of gas-phase HNO_3 to a deliquescent layer coating the mineral dust particle can increase the amount of bioavailable and soluble iron.[16] Furthermore, it has been recently proposed that the amount of bioavailable iron can depend on particle size[17] and that iron nanoparticles can form in the atmosphere through cloud processing.[18] Given that particle size and iron oxide nanoparticles in particular may play a role in the chemistry of the atmosphere, we investigate here the size-dependent, light-initiated redox chemistry of goethite, α-FeOOH, in low-pH environments.

Lastly, in light of the fact that metal-containing anthropogenic dusts are becoming an increasing source of metals in the atmosphere, it is important to identify all possible sources of these dusts. We discuss the potential for nanodust, dust produced during production of engineered nanomaterials, to become an emerging source of metal-containing anthropogenic dust in the atmospheric environment.[7] Recent inventories have shown that metal and metal-oxide-based nanomaterials are a large component of materials being used in consumer products. Therefore, it is reasonable to hypothesize that metal-containing engineered nanomaterials have the greatest chance to make their way into the atmospheric environment. Furthermore, engineered nanoparticles have the potential for very different and size-dependent physical, chemical, and biological properties compared to larger-sized particles.[19] Presented here is the dissolution of metal nanoparticles in low-pH environments and a comparison of the reactivity to larger-sized particles.

Recent inventories have shown that metal and metal-oxide-based nanomaterials are a large component of materials being used in consumer products. Therefore, it is reasonable to hypothesize that metal-containing engineered nanomaterials have the greatest chance to make their way into the atmospheric environment.

Photochemistry of Adsorbed Nitrate as a Renoxification Mechanism. Reactions of nitrogen oxides with mineral dust lead to the formation of adsorbed nitrate, nitrate coatings, and deliquesced nitrate layers on the surface of the dust particles. Given that nitrate is an important chromophore in natural waters and in snowpacks,[20] we have begun to investigate the photochemistry of adsorbed nitrate on the surface of aluminum oxide particles as a proxy to better understand the day time chemistry of nitrate-coated mineral dust in the atmosphere. In earlier studies, we have shown that irradiation with broad-band light (wavelengths between 300 and 700 nm) results in a loss of adsorbed nitrate on the particle surface with the concomitant formation of gas-phase products including NO_2, NO, and N_2O.[21,23] In the current study, we focus our

DOI: 10.1021/jz100371d | J. Phys. Chem. Lett. 2010, 1, 1729–1737

THE JOURNAL OF PHYSICAL CHEMISTRY Letters

PERSPECTIVE

pubs.acs.org/JPCL

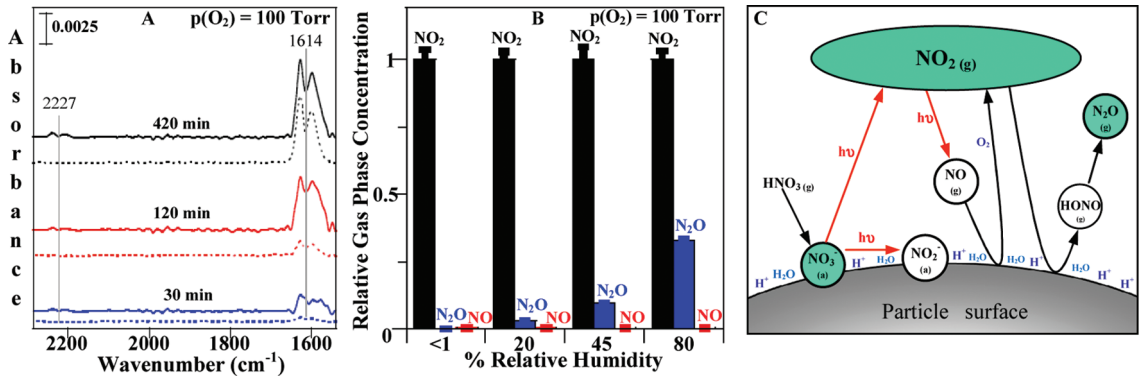

Figure 2. (A). FTIR spectra of gas-phase products formed during photolysis of adsorbed nitrate at 310 ± 10 nm; %RH < 1 (dash line) and 45 (solid line) at 298 K. (B). Relative gas-phase concentrations obtained from FTIR spectra following irradiation of adsorbed nitrate in the presence of molecular oxygen at 298 K under different relative humidity (%RH) conditions (< 1, 20, 45, and 80) after 420 min of irradiation time. Gas-phase concentrations have been normalized to the largest gas-phase product species NO_2. (C). Proposed reaction mechanism to account for various products (green indicates species detected; white indicates proposed intermediate).

attention on the gas-phase products that form in this reaction upon narrow-band photolysis (310 ± 10 nm) of adsorbed nitrate near the wavelength maximum of the first electron transition ($n \rightarrow \pi^*$) to better understand the potential role of nitrate photochemistry on mineral dust.

FTIR spectra of gas-phase products formed during the narrow-band photolysis of adsorbed nitrate in the presence of 100 Torr of molecular oxygen are shown in Figure 2A. The solid lines show the gas-phase spectra at 45% relative humidity (RH) compared to dry conditions (%RH < 1). Under dry conditions, that is, in the absence of gas-phase and adsorbed water, NO_2 is the sole gas-phase product observed with a characteristic absorption at 1614 cm^{-1}, whereas under humid conditions of 45% RH, gas-phase N_2O is also formed, as seen by the absorption band at 2227 cm^{-1} in addition to NO_2. The relative gas-phase concentrations, following 420 min of 310 nm band-pass irradiation in the presence of molecular oxygen under different RH conditions (RH < 1, 20, 45, and 80%) are shown Figure 2B. The gas-phase concentrations have been normalized to the largest gas-phase product species observed after 420 min of irradiation at a given RH, which in all cases is found to be NO_2. Moreover, N_2O production is increased at the highest RH conditions. The percentage yields of N_2O formation were $(2.1 \pm 0.1) \times 10^{-3}$, $(4.4 \pm 0.1) \times 10^{-3}$, $(5.4 \pm 0.2) \times 10^{-3}$, and $(10.1 \pm 0.5) \times 10^{-3}$ for %RH < 1, 20, 45, and 80, respectively. There is no detectable NO production under all experimental conditions.

From previous studies on nitrate photochemistry in the solution phase and snowpack, it is well-known that irradiation of the nitrate ion with light at ~305 nm yields nitrogen dioxide and nitrite according to reactions 1 and 2[20,23−26]

$$NO_3^- + H^+ \xrightarrow{305\ nm} NO_2 + OH \qquad (1)$$

and

$$NO_3^- \xrightarrow{305\ nm} NO_2^- + O(^3P) \qquad (2)$$

Here, we can easily detect the NO_2 photoproduct in the gas phase. At higher RH, a significant amount of N_2O was observed. Several studies have focused on the heterogeneous formation of N_2O from the hydrolysis of gas-phase NO_2 via HONO on acidic and oxide surfaces.[27,28] The net reaction yields N_2O and HNO_3, which can potentially readsorb on the surface if sites are available.

$$8NO_2 + 3H_2O \xrightarrow{[H+]} N_2O + 6HNO_3 \qquad (3)$$

The experimental data can be explained by this mechanism, and the reason why there is an increase in N_2O formation under humid conditions is due to secondary reactions of gas-phase NO_2 on the acidic oxide surface. Therefore, the current results under dry and humid conditions can be explained in the framework of nitrate ion photochemistry to yield NO_2 followed by heterogeneous hydrolysis of gas-phase NO_2 on acidic surfaces to yield N_2O as a product.

The schematic of the proposed reaction mechanism of photolysis of adsorbed nitrate at 310 nm is shown in Figure 2C. Heterogeneous uptake of gas-phase nitric acid, HNO_3(g), on the left side of the diagram, yields nitrate ion (NO_3^-) and protons (H^+) on the surface in the presence and absence of coadsorbed water. Upon 310 nm irradiation, NO_2 is produced as the primary gas-phase product. Furthermore, the photochemistry of gas-phase NO_2 yields NO, which can possibly change the gas-phase product distribution. In a reaction cell with only gas-phase NO_2 present, photolysis is measured and determined to be 40-fold faster than that of adsorbed nitrate photolysis. In the presence of an oxide surface and molecular oxygen, gas-phase NO is oxidized back to NO_2 via a surface-catalyzed oxidation reaction yielding no detectable NO in the gas phase. In the presence of coadsorbed water, NO_2 becomes the precursor for the gas-phase N_2O through heterogeneous hydrolysis of NO_2 on the acid surface.

The kinetics of the reaction is also seen to change as a function of relative humidity. The saturated nitrate coverage on the alumina surface at $t = 0$ was $7 \pm 1 \times 10^{14}$ molec/cm^2. The rate of nitrate loss upon 310 nm irradiation was monitored more as a function of time for the first 90 min as measured by the decrease in the integrated absorbance of the NO_3^- ν_3 band.[20] Assuming first-order kinetics, the apparent rate constants obtained at different % RH were $(0.5 \pm 0.1) \times 10^{-5}$, $(1.9 \pm 0.2) \times 10^{-5}$, $(1.4 \pm 0.1) \times 10^{-5}$, and $(1 \pm 0.1) \times 10^{-5}$ s^{-1} for RH < 1, 20, 45 and 80%, respectively. Thus, the initial rate of

DOI: 10.1021/jz100371d | J. Phys. Chem. Lett. 2010, 1, 1729–1737

photolysis of adsorbed nitrate at 310 nm is approximately 2- to 4-fold faster under humid conditions compared to dry conditions. On the basis of calculated photolysis rate constants for HNO_3 and the reported values in the literature,[29] the 310 nm photolysis of adsorbed nitrate on the aluminum oxide particle surface is significantly increased relative to the HNO_3 photolysis rate constant of $\sim 7 \times 10^{-7}$ s^{-1} in the gas phase. Furthermore, Zhu et al. showed that absorption cross sections for adsorbed nitric acid were nearly 4 times greater compared to those of nitric acid in the gas phase.[30] These results highlight the significance of involvement of the atmospheric particle surface in renoxification initiated by light.

The higher loss of surface nitrate under humid conditions can be attributed to several factors. Primarily, formation of inner- and outer-sphere complexes of nitrate ion following the reaction with coadsorbed water decreases the direct interaction with the surface and leads to less molecular distortion from the planar D_{3h} symmetry of the free ion compared to the oxide coordinated nitrate structures present under dry conditions. Miller and Grassian showed that coadsorbed water affects the energetics of the $n \rightarrow \pi^*$ electronic transition near 300 nm, with a red shift resulting in a higher overlap of the absorption profile of nitrate with solar wavelengths.[31] Clearly, adsorbed water can play an important role in the photochemistry of adsorbed species. Moreover, the gradual decrease of net nitrate loss from the surface at higher relative humidies (%RH > 20) can be attributed to the readsorption of HNO_3 from reaction 3 on to the particle surface.

Surface Photochemistry as a Mechanism for SO_2 Oxidation to Sulfate. As already noted, mechanisms for SO_2 oxidation on mineral dust surfaces are not well-understood. TiO_2 is a well-known photocatalyst, and recently, it has been suggested that there are sufficient amounts of TiO_2 in mineral dust for it to play a role in the chemistry of the atmosphere.[32,33] Here, we investigate the oxidation of SO_2 to yield adsorbed sulfate on TiO_2, a light-absorbing component of mineral dust.

In these experiments, following the adsorption of SO_2 under different environmental conditions of relative humidity, molecular oxygen, and broad-band irradiation, the TiO_2 particles are transferred into an ultrahigh vacuum chamber for analysis with X-ray photoelectron spectroscopy (XPS).

Figure 3 shows high-resolution XPS data in the S2p region of TiO_2 particle surfaces following SO_2 adsorption under different environmental conditions. On the basis of the high-resolution XPS data collected for standards, the peaks observed in Figure 3 can be assigned to two sets of doublets. One set, at higher binding energy, is centered at 170.7 and 169.5 eV. This doublet is assigned to the $S2p_{1/2}$ and $S2p_{3/2}$, respectively, of sulfate groups, SO_4^{2-}, on the surface. Another set of doublets observed at lower binding energy is centered at 169 and 167.8 eV and assigned to the $S2p_{1/2}$ and $S2p_{3/2}$ transitions for adsorbed sulfite, SO_3^{2-}. The difference in the energetics of the $S2p_{3/2}$ transition between adsorbed sulfate and sulfite is 1.7 eV, close to that of standards previously measured and earlier studies of SO_2 adsorption on oxide surfaces.[34−36]

Following exposure of TiO_2 particles to SO_2, or SO_2 and O_2, only one species is observed on the surface, as seen in the S2p region. On the basis of the peak positions, this species is identified as adsorbed sulfite. While adsorbed sulfite is the sole

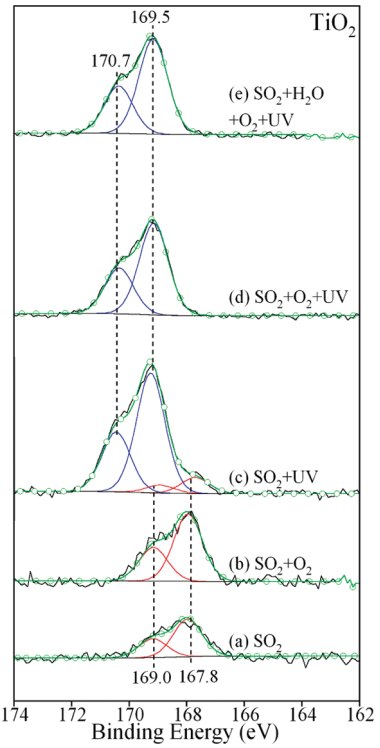

Figure 3. High-resolution XPS data in the S2p region following TiO_2 particle exposure to SO_2 at 298 K of (a) 100 mTorr of SO_2, (b) 100 mTorr of SO_2 and 100 Torr of O_2, (c) 100 mTorr of SO_2 in the presence of UV light, (d) 100 mTorr of SO_2 and 100 Torr of O_2 in the presence of UV light, and (e) 100 mTorr of SO_2, 13 Torr of H_2O, and 100 Torr of O_2 in the presence of UV light. The spectra are fit to two transitions, $S2p_{3/2}$ and $S2p_{1/2}$, for two species, adsorbed sulfite and sulfate (see text for further details). The individual components are shown in red (sulfite) and blue (sulfate) solid lines. The total peak fit is shown in green with circular markers. The wavelength of light used was $\lambda > 300$ nm.

adsorbed product observed in the absence of light, there was a change in the adsorbed product species when the sample was irradiated with broad-band light ($\lambda > 300$ nm) during adsorption (Figure 3C−E). In particular, a higher-energy doublet appeared in the S2p region associated with adsorbed sulfate.

The photoconversion to sulfate occurs even in the absence of molecular oxygen and water. However, in the absence of another source of oxygen, such as O_2 and H_2O, there is still a small amount of sulfite observed when samples are exposed to SO_2 only in the presence of UV light. Since there is no additional source of oxygen during this reaction, oxygen from surface oxygen sites and/or other SO_2 molecules are available for sulfate formation. In the presence of H_2O vapor and molecular oxygen, irradiation results in the full conversion to sulfate.

It has been proposed that reactive hydroxyl radicals in the environment can react with HSO_3^- and SO_3^{2-} species, converting S(IV) to sulfate in cloudwater.[37] Formation of the SO_3^- radical is proposed via the following pathway

$$OH + HSO_3^- \rightarrow SO_3^- + H_2O \quad (4)$$

$$OH + SO_3^{2-} \rightarrow SO_3^- + OH^- \quad (5)$$

DOI: 10.1021/jz100371d | J. Phys. Chem. Lett. 2010, 1, 1729–1737

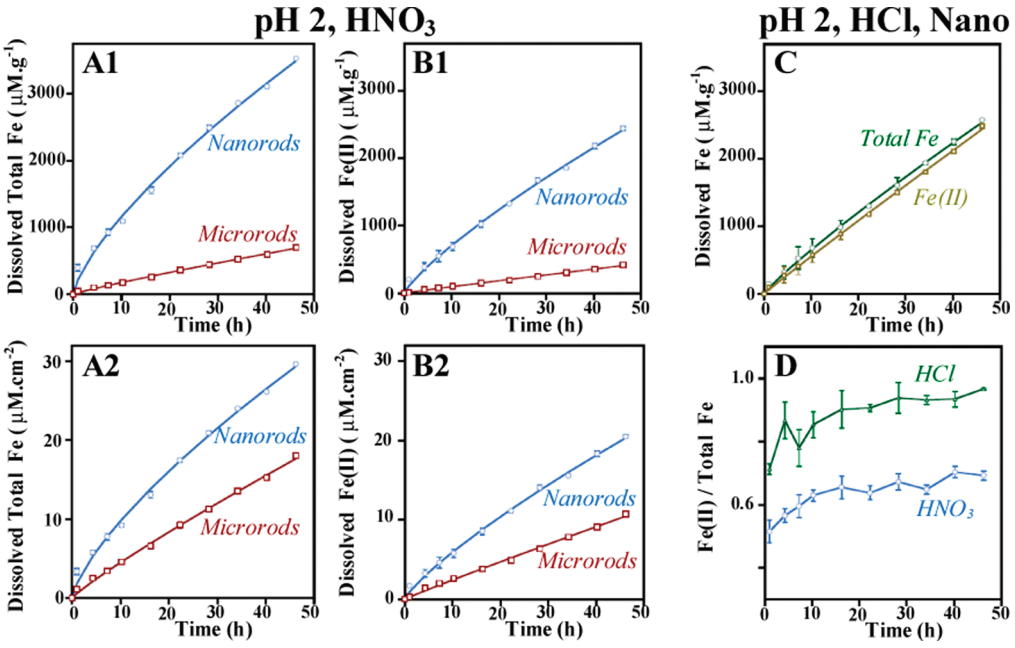

Figure 4. The dissolution of rod-shaped α-FeOOH particles is monitored by the formation of total soluble Fe and Fe(II) in solutions of 0.01 N HNO_3 and HCl (pH 2.0). These plots compare the dissolution of nanorods to that of microrods in the irradiated systems. Data are shown for both total Fe [Fe(II) and Fe(III)] and Fe(II) only in HNO_3 concentrations and are normalized to both particle mass (A1, B1) and surface area (A2, B2). The data for the dissolved total Fe [Fe(II) and Fe(III)] and Fe(II) only for nanorods suspendend in solutions acidified with HCl are shown in (C). A comparison of the Fe(II) fraction with respect to total iron dissolution is shown in (D).

SO_3^- radical formation can be followed by the recombination with molecular oxygen, which results in SO_5^- formation (reaction 6)

$$SO_3^- + O_2 \rightarrow SO_5^- \quad (6)$$

The resulting SO_5^- can be involved in many reactions, some of which result in the formation of SO_4^{2-} species

$$SO_5^- + SO_3^{2-} \rightarrow SO_4^- + SO_4^{2-} \quad (7)$$

TiO_2 surfaces are truncated with adsorbed hydroxyl groups from the dissociation of adsorbed water. In the presence of UV light, these can be converted to highly reactive hydroxyl radicals from the reaction of water at photoinduced valence band holes that interact with SO_2 adsorption products to form oxidized species on the surface such as adsorbed sulfate. Although direct evidance for this mechanism has yet to be established, these laboratory studies point to a new route for SO_2 oxidation on mineral dust particles containing titanium dioxide and may be operative on other metal oxides from both natural and anthropogenic sources as well.

Size-Dependent Dissolution of α-FeOOH in Low-pH Environments. The dissolution of goethite, α-FeOOH, is of great interest, and in this laboratory investigation, we have compared the dissolution results of α-FeOOH nanorods to larger microrods in order to determine if there are any size-dependent effects beyond surface area differences. In our recent published work on iron dissolution, we have shown an enhancement factor of ~3 for nanorod dissolution under dark conditions compared to microrods at pH 2, even after normalizing to surface area differences, when particles are isolated and not in an aggregated state.[38]

Perhaps of greater interest in the atmosphere is the size-dependent nanoscale redox chemistry of α-FeOOH in the presence of light.[39] Figure 4A1 and A2 shows a comparison of dissolution data taken at pH 2.0 under irradiation ($\lambda >$ 300 nm) for nanorods and microrods. These data are plotted on both a per mass (A1) and a per surface area (A2) basis. These data show that total iron dissolution in the presence of light is enhanced by ~2 for nanorods compared to that for microrods. Furthermore, these data reveal that nearly half of the dissolved iron is Fe(II), as shown in (B1) and (B2). In good agreement to these data, field experiments have reported that the increasing concentration of Fe(II) observed results from photochemical production during the period of greatest sunlight intensity.[40]

Furthermore, significant differences can be seen in the ratio of Fe(II) to total Fe dissolution between nanorods and microrods. During the 46 h of dissolution, the rate changes and levels off with an Fe(II) fraction of ~0.7 for nanorods and ~0.5 for microrods. Therefore, the Fe(II) production in nanorods is considerably higher than that observed for microrods, especially at longer time scales.

In irradiated systems, photogenerated electron−hole (e^-/h^+) pairs on the semiconductor surfaces lead the redox process. In addition to the above mechanism, in systems with no organic ligands for surface complexation, surface hydroxide play a major role in Fe(III)/Fe(II) redox reactions via donating electrons to a photoexited Fe(III) surface atom, yielding a surface-bound Fe(II) atom followed by a detachment of Fe(II) to the solution.[41] According to previous studies,[42] strong absorption bands at 3489 and 3661 cm^{-1} in FTIR spectroscopy are evidence for the higher density of O−H groups on nanorod

DOI: 10.1021/jz100371d | J. Phys. Chem. Lett. 2010, 1, 1729–1737

surfaces compared to that on microrods. Therefore, the observed enhancement in Fe(II) production in nanorods may be due to having more reactive faces, that is, the (021) face, with higher density of surface O−H groups. In acidic surface waters, photoinduced reductions of Fe(III) to Fe(II) are key and serve to increase the solubility of aerosol Fe.[43,44] On the basis of these facts, we can conclude that the production of soluble Fe(II) increases in the presence of light, and this is further enhanced [Fe(II) and total Fe] for nanoscale particles.

Data for total iron dissolution and dissolved Fe(II) from nanorods with 0.01 N HCl (pH 2) under irradiated conditions are shown in Figure 4C. These experiments were undertaken to investigate the effect of acid anion on iron dissolution. It can be clearly seen that Cl^- yields lower total iron dissolution compared to NO_3^-, whereas dissolved Fe(II) concentrations with HNO_3 and HCl are found to be similar. Moreover, as seen in Figure 4D, for suspensions acidified with HCl, the Fe(II) to total iron ratio is one, indicating that all of the dissolved iron present in the suspension is present as Fe(II), whereas for NO_3^-, this fraction is ~0.6. The difference in total iron dissolution between the two anions can be attributed to several factors. For example, the strength and mode of anion adsorption and the ability of the complex to be further protonated can cause differences. Polyatomic oxyanions, such as nitrate, are capable of binding in different adsorption modes to the surface, including a bidentate and bridging coordination mode, which chloride is unable to form. Thus, the difference in total iron dissolution may be related to the mode of adsorption and the ability to form certain surface complexes.[39]

Additionally, in Cl^--containing suspensions, $[Fe(OH_2)_5Cl]^{2+}$ and $[Fe(OH_2)_4Cl_2]^+$ coexist at low pHs, where the former is the dominant species at ~pH 1[45−47] and these chloride-containing iron species are photoactive in UV and visible regions of the solar spectrum. According to Hsu et al., $[Fe(OH_2)_5Cl]^{2+}$ is photoreduced to $[Fe(OH_2)_6]^{2+}$ according to[47]

$$[Fe(OH_2)_5(Cl)]^{2+} + H_2O + h\nu \rightarrow [Fe(OH_2)_6]^{2+} + Cl^{\bullet} \quad (8)$$

On the basis of the above facts and the data presented, it can be proposed that the higher rate of Fe(II) production in Cl^- suspensions may be due to formation of Fe(III)−Cl complexes. In HNO_3 suspensions, NO_3^- does not readily form solution-phase iron complexes, leaving $[Fe(OH_2)_6]^{3+}$ and $[Fe(OH_2)_5(OH)]^{2+}$ as dominant species. Nitrate also can yield $OH^{\bullet}$ via eq 1, which reoxidizes Fe(II) back to Fe(III). In addition, photolysis of $[Fe(OH_2)_5(OH)]^{2+}$ efficiently yields $OH^{\bullet}$ radicals. Therefore, it can be suggested that the higher $OH^{\bullet}$ concentration originating from the photolysis of both NO_3^- and $[Fe(OH_2)_5(OH)]^{2+}$ results in a faster oxidation of $[Fe(OH_2)_6]^{2+}$ back to $[Fe(OH_2)_6]^{3+}$ and, thus, a lower Fe(II) fraction compared to Cl^- suspensions.

Nanodust: Engineered Nanomaterials as a New Source of Metal-Containing Anthropogenic Dusts. Although mineral dust aerosol is a well-known and natural source of metals in the atmosphere, there is increasing evidence that there is an even larger number of anthropogenic sources of metal-containing aerosols present in the troposphere. From nanometal oxides to nanoclays to nanocalcium carbonate, there is a range of minerals that have been engineered on the nanoscale and are commercially available. Particle sizing instruments detect airborne particles on the nanoscale but are often unable to distinguish ultrafine particles from gas-phase nucleation processes or from engineered nanomaterials. Compositional information is necessary to ascertain the source of airborne nanoparticles. A field study conducted in Houston was one of the first to report detection of an ambient airborne nanomaterial (10 nm SiO_2) attributed to an anthropogenic source.[48]

Due to the rapid and sustained growth of nanotechnology, that is, more than 800 consumer products that contain engineered nanomaterials and the fact that nearly 50% contain metal or a metal oxide composite (http://www.nanotechproject.org/inventories/consumer), the question can be posed, is nanodust, defined as dust with at least one dimension less than 100 nm produced from industrial sources, a new source of metal-containing dust in the atmosphere? Interestingly, some recent studies have focused on investigating the relative "dustiness" of nanomaterials, defined as the propensity of a material to generate airborne dust. Comparison between nanoscale TiO_2 and bulk TiO_2 showed that nano-TiO_2 had the highest dustiness of nine tested minerals, while bulk TiO_2 had the lowest.[49] Other studies also suggest that nanomaterials have a greater propensity to become airborne compared with larger-sized particles.[50] Recent studies have shown that TiO_2 exhibits interesting photochemistry, including photoconversion of NO_2 to HONO and O_3 photodecomposition.[51,52]

Is nanodust, defined as dust with at least one dimension less than 100 nm produced from industrial sources, a new source of metal-containing dust in the atmosphere ?

Because of its antimicrobial properties, silver-based nanomaterials alone account for nearly one-third of the commercially manufactured products. In a follow-up to our investigations discussed above for iron oxide dissolution in low-pH environments, here, we investigate the dissolution behavior of nanoscale silver compared with microscale silver as a function of pH so as to begin to ascertain the propensity for dissolution upon reactions with acidic gases in the atmosphere.

Silver dissolution in nitric acid is a well-known chemical reaction according to[53]

$$3Ag + 4HNO_3 \rightarrow 3AgNO_3 + NO + 2H_2O \quad (9)$$

Larger-sized (10−800 μm) silver particles do not dissolve to any great extent in nitric acid until the acid concentration is

DOI: 10.1021/jz100371d | J. Phys. Chem. Lett. 2010, 1, 1729–1737

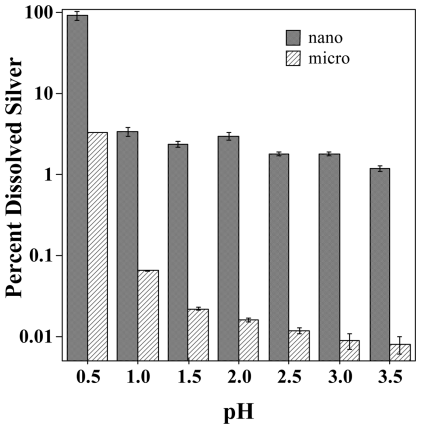

Figure 5. Comparison of Ag nanoparticle dissolution at low pH to that of larger, micrometer-sized particles.

~4 M. Figure 5 shows the results of a comparison of silver nanoparticle dissolution compared to silver microparticle dissolution in low-pH environments.

The silver nanoparticles and silver microparticles were purchased in powder form from Nanostructured and Amorphous Materials, Inc. (Houston, TX) and Aldrich (St. Louis, MO), respectively. Details of experimental methods and characterization of the silver nanoparticles in neutral and low-pH nitric acid conditions can be found in Elzey and Grassian.[54] Briefly, both silver samples were suspended in neutral and low-pH nitric acid solutions at a concentration of 1 wt % Ag. Upon removal of the particles (see ref 51), inductively coupled plasma optical emission spectroscopy (ICP/OES) analysis of the solution phase was used to determine the percent of silver dissolved. Analysis of these data show that compared to micrometer-sized particles, silver nanoparticle dissolution is orders of magnitude greater in the pH range from 3.5 to 0.5. At the lowest pH of 0.5, nearly 100% of the nanosilver is found to dissolve. These data show that silver nanoparticles dissolve completely in acidic concentrations ~10 times weaker than the concentration required for dissolution of bulk silver particles, demonstrating unique, size-dependent dissolution behavior for silver nanoparticles. Although differences in rates are expected due to surface area and surface free energy considerations, the significant increase in the extent of dissolution for the nanoparticles in acidic solution confirms that engineered metal and a metal oxide nanomaterials have the potential to behave as a distinctive dust component, nanodust, in the atmospheric environment. Low-pH environments from heterogeneous reactions of nanomaterials with nitric acid, or other acidic gases in the atmosphere, can lead to soluble forms of metal nanoparticles that upon deposition can be ecologically damaging or harmful to aquatic species in water systems. It is clear from recent studies that nanoscale materials in general are chemically distinct compared to larger micrometer-sized particles and that silver nanoparticles in particular have size-dependent redox chemistry[55,56] that will be especially important in the behavior of these particles in the environment.

Future Prospects — Physical Chemistry of Reactions on Atmospheric Dusts. In this Perspective, we discussed several potentially important reactions on mineral dust and on nanodust, a possible new source of metal-containing dusts in the atmosphere from industrial sources such as engineered nanomaterials. These reactions can impact atmospheric chemistry in ways that are only beginning to be fully understood. A further understanding of how these processes play a role in the atmospheric environment will ultimately require integration of field measurements, atmospheric modeling, and laboratory studies.

From a physical chemistry perspective, many questions remain unanswered, and many issues remain unresolved as to the molecular details of heterogeneous surface photochemistry and size-dependent nanoscale redox chemistry. These include understanding mechanistic details of primary and secondary surface photoprocesses, electronic excited states for adsorbed molecules, quantum yields, and time scales of the fundamental detailed steps in these reactions. As discussed recently by Finlayson-Pitts,[57] a molecular-level understanding can only be gained by fully integrating experiment and theory to elucidate these complex systems. Furthermore, the size-dependent chemical reactivity of nanoparticles is of great interest from many perspectives, but here, as it relates to reactions with trace atmospheric gases and the changes in the properties of the particles that could not be predicted from the behavior of larger particles. Other new areas of note include heterogeneous stereochemistry, as recently discussed by Geiger and co-workers.[58]

By bringing to bear the tools and methods of physical chemistry, including nonlinear laser spectroscopy, synchrotron-based spectroscopy, chemical kinetics, theory of electronic excited states, surface science and nanoscience, physical chemistry can provide some important insights into the details of these reactions. From which a much-needed understanding of the properties and anthropogenic activities that impact the Earth's atmosphere and terrestrial and aquatic ecosystems through deposition on a detailed molecular level can be gained.

AUTHOR INFORMATION

Corresponding Author:

*To whom correspondence should be addressed.

Biographies

Gayan Rubasinghege is a graduate student at the University of Iowa in the Department of Chemistry. His research interests are in heterogeneous chemistry and photochemistry of mineral dust aerosol. In 2010, he received first prize in the Jakobsen Graduate Conference held on the University of Iowa campus. He plans to graduate in 2011.

Sherrie Elzey is a graduate student at The University of Iowa in the Department of Chemical and Biochemical Engineering. She currently has a NDSEG fellowship and will receive her Ph.D. in May 2010. Her current work focuses on the physicochemical properties of nanomaterials as they relate to environmental, health, and safety studies.

Jonas Baltrusaitis is an Assistant Research Scientist. His research interests involve heterogeneous catalysis and photocatalysis of trace atmospheric gases in the atmosphere. He received the Graduate Deans' Distinguished Dissertation Award at the University of Iowa in 2009.

DOI: 10.1021/jz100371d | J. Phys. Chem. Lett. 2010, 1, 1729–1737

Pradeep M. Jayaweera is a Professor, Department of Chemistry, University of Sri Jayewardenepura, Sri Lanka. His main research interests involve solar energy conversion, Raman, surface-enhanced Raman, excited-state properties of metal complexes, and surface chemistry of nanoparticles.

Vicki H. Grassian is a Professor in the Department of Chemistry and the Director of the Nanoscience and Nanotechnology Institute at the University of Iowa. Her research interests are in heterogeneous atmospheric chemistry, climate impact of aerosols, environmental molecular surface science, and environmental and health aspects of nanoscience and nanotechnology. For more information, see: http://www.chem.uiowa.edu/faculty/grassian/index.html.

ACKNOWLEDGMENT Although the research described in this article has been funded wholly or in part by the EPA through Grant EPA R83389101-0 to V.H.G. (silver nanoparticle dissolution), it has not been subjected to the Agency's required peer and policy review and therefore does not necessarily reflect the views of the Agency, and no official endorsement should be inferred. This material is also based upon work supported by the National Science Foundation under Grants EAR0506679 (iron dissolution) and CHE0952605 (surface photochemistry of adsorbed nitrate and sulfur dioxide oxidation). S.E. acknowledges support by the DoD through the NDSEG program. The authors would like to thank Professors Michelle Scherer, Gregory Carmichael, and Mark Young for helpful discussions during the course of this work.

REFERENCES

(1) Dentener, F. J.; Carmichael, G. R.; Zhang, Y.; Lelieveld, J.; Crutzen, P. J. Role of Mineral Aerosol as a Reactive Surface in the Global Troposphere. *J. Geophys. Res., Atmos.* **1996,** *101*, 22869–22889.

(2) Usher, C. R.; Michel, A. E.; Grassian, V. H. Reactions on Mineral Dust. *Chem. Rev.* **2003,** *103*, 4883–4939.

(3) Cwiertny, D. M.; Young, M. A.; Grassian, V. H. Chemistry and Photochemistry of Mineral Dust Aerosol. *Annu. Rev. Phys. Chem.* **2008,** *59*, 27–51.

(4) Sullivan, R. C.; Guazzotti, S. A.; Sodeman, D. A.; Prather, K. A. Direct Observations of the Atmospheric Processing of Asian Mineral Dust. *Atmos. Chem. Phys.* **2007,** *7*, 1213–1236.

(5) Higashi, M.; Takahashi, Y. Detection of S(IV) Species in Aerosol Particles Using XANES Spectroscopy. *Environ. Sci. Technol.* **2009,** *43*, 7357–7363.

(6) Hwang, H.; Ro, C. U. Direct Observation of Nitrate and Sulfate Formations from Mineral Dust and Sea-Salts using Low-Z Particle Electron Probe X-ray Microanalysis. *Atmos. Env.* **2006,** *40*, 3869–3880.

(7) Laskin, A.; Iedema, M. J.; Ichkovich, A.; Graber, E. R.; Taraniuk, I.; Rudich, Y. Direct Observation of Completely Processed Calcium Carbonate Dust Particles. *Farad. Discuss.* **2005,** *130*, 453–468.

(8) Gidney, J. T.; Twigg, M. V.; Kittelson, D. B. Effect of Organometallic Fuel Additives on Nanoparticle Emissions from a Gasoline Passenger Car. *Environ. Sci. Technol.* **2010,** *44*, 2562–2569.

(9) Adachi, K.; Buseck, P. R. Hosted and Free-Floating Metal-Bearing Atmospheric Nanoparticles in Mexico City. *Environ. Sci. Technol.* **2010,** *44*, 2299–2304.

(10) Grassian, V. H. New Directions: Nanodust — A Source of Metals in the Atmospheric Environment? *Atmos. Environ.* **2009,** *43*, 4666–4667.

(11) Vaida, V. Spectroscopy of Photoreactive Systems: Implications for Atmospheric Chemistry. *J. Phys. Chem. A* **2009,** *113*, 5–18.

(12) Usher, C. R.; Al-Hosney, H.; Carlos-Cuellar, S.; Grassian, V. H. A Laboratory Study of the Heterogeneous Uptake and Oxidation of Sulfur Dioxide on Mineral Dust Particles. *J. Geophys. Res., Atmos.* **2002**, *107*, doi:10.1029/2002JD002051.

(13) Li, L.; Chen, Z. M.; Zhang, Y. H.; Zhu, T.; Li, S.; Li, H. J.; Zhu, L. H.; Xu, B. Y. Heterogeneous Oxidation of Sulfur Dioxide by Ozone on the Surface of Sodium Chloride and its Mixtures with Other Components. *J. Geophys. Res.* **2007,** *112*, D18301.

(14) Jickells, T. D.; An, Z. S.; Andersen, K. K.; Baker, A. R.; Bergametti, G.; Brooks, N.; Cao, J. J.; Boyd, P. W.; Duce, R. A.; Hunter, K. A.; et al. Global Iron Connections Between Desert Dust, Ocean Biogeochemistry and Climate. *Science* **2005,** *308*, 67–71.

(15) Matsumoto, J.; Takahashi, K.; Matsumi, Y.; Yabushita, A.; Shimizu, A.; Matsui, I.; Sugimoto, N. Scavenging of Pollutant Acid Substances by Asian Mineral Dust Particles. *Geophys. Res. Lett.* **2006,** *33*, L07816.

(16) Meskhidze, N.; Chameides, W. L.; Nenes, A. Dust and Pollution: A Recipe for Enhanced Ocean Fertilization? *J. Geophys. Res., Atmos.* **2005,** *110*, D03301.

(17) Baker, A. R.; Jickells, T. D. Mineral Particle Size as a Control on Aerosol Iron Solubility. *Geophys. Res. Lett.* **2006,** *33*, L17608.

(18) Shi, Z.; Krom, M. D.; Bonneville, S.; Baker, A. R.; Jickells, T. D.; Benning, L. G. Formation of Iron Nanoparticles and Increase in Iron Reactivity in Mineral Dust During Simulated Cloud Processing. *Environ. Sci. Technol.* **2009,** *43*, 6592–6596.

(19) Grassian, V. H. When Size Really Matters: Size-Dependent Properties and Surface Chemistry of Metal and Metal Oxide Nanoparticles in Gas and Liquid Phase Environments. *J. Phys. Chem. C* **2008,** *112*, 18303–18313.

(20) Grannas, A. M.; Jones, A. E.; Dibb, J.; Ammann, M.; Anastasio, C.; Beine, H. J.; Bergin, M.; Bottenheim, J.; Boxe, C. S.; Carver, G.; et al. An Overview of Snow Photochemistry: Evidence, Mechanisms and Impacts. *Atmos. Chem. Phys.* **2007,** *7*, 4329–4373.

(21) Rubasinghege, G.; Grassian, V. H. Photochemistry of Adsorbed Nitrate on Aluminum Oxide Particle Surfaces. *J. Phys. Chem. A* **2009,** *113*, 7818–7825.

(22) Schuttlefield, J.; Rubasinghege, G.; El-Maazawi, M.; Bone, J.; Grassian, V. H. Photochemistry of Adsorbed Nitrate. *J. Am. Chem. Soc.* **2008,** *130*, 12210–12211.

(23) Goldstein, S.; Rabani, J. Mechanism of Nitrite Formation by Nitrate Photolysis in Aqueous Solutions: The Role of Peroxynitrite, Nitrogen Dioxide, and Hydroxyl Radical. *J. Am. Chem. Soc.* **2007,** *129*, 10597–10601.

(24) Chu, L.; Anastasio, C. Quantum Yields of Hydroxyl Radical and Nitrogen Dioxide from the Photolysis of Nitrate on Ice. *J. Phys. Chem. A* **2003,** *107*, 9594–9602.

(25) Mack, J.; Bolton, J. R. Photochemistry of Nitrite and Nitrate in Aqueous Solution: A Review. *J. Photochem. Photobiol., A* **1999,** *128*, 1–13.

(26) Zellner, R.; Exner, M.; Herrmann, H. Absolute OH Quantum Yields in the Laser Photolysis of Nitrate, Nitrite and Dissolved H_2O_2 at 308 and 351 nm in the Temperature-Range 278−353 K. *J. Atmos. Chem.* **1990,** *10*, 411–425.

(27) Wiesen, P.; Kleffmann, J.; Kurtenbach, R.; Becker, K. H. Mechanistic Study of the Heterogeneous Conversion of NO_2 into HONO and N_2O on Acid Surfaces. *Farad. Discuss.* **1995,** *100*, 121–127.

(28) Finlayson-Pitts, B. J.; Wingen, L. M.; Sumner, A. L.; Syomin, D.; Ramazan, K. A. The Heterogeneous Hydrolysis of NO_2 in Laboratory Systems and in Outdoor and Indoor Atmospheres: An Integrated Mechanism. *Phys. Chem. Chem. Phys.* **2003,** *5*, 223–242.

(29) Finlayson-Pitts, B. J.; Pitts, J. J. N. *Chemistry of the Upper and Lower Atmosphere—Theory, Experiments, and Applications*; Academic Press: San Diego, CA, 2000.

(30) Zhu, C.; Xiang, B.; Chu, L. T.; Zhu, L. 308 nm Photolysis of Nitric Acid in the Gas Phase, on Aluminum Surfaces, and on Ice Films. *J. Phys. Chem. A* **2010,** *114*, 2561–2568.

(31) Miller, T. M.; Grassian, V. H. Heterogeneous Chemistry of NO_2 on Mineral Oxide Particles: Spectroscopic Evidence for Oxide-Coordinated and Water-Solvated Surface Nitrate. *Geophys. Res. Lett.* **1998,** *25*, 3835–3838.

(32) Ndour, M.; D'Anna, B.; George, C.; Ka, O.; Balkanski, Y.; Kleffmann, J.; Stemmler, K.; Ammann, M. Photoenhanced Uptake of NO_2 on Mineral Dust: Laboratory Experiments and Model Simulations. *Geophys. Res. Lett.* **2008,** *35*, L05812.

(33) Ndour, M.; Nicolas, M.; D'Anna, B.; Ka, O.; George, C. Photoreactivity of NO_2 on Mineral Dusts Originating from Different Locations of the Sahara Desert. *Phys. Chem. Chem. Phys.* **2009,** *11*, 1312–1319.

(34) Smirnov, M. Y.; Kalinkin, A. V.; Pashis, A. V.; Sorokin, A. M.; Noskov, A. S.; Kharas, K. C.; Bukhtiyarov, V. I. Interaction of Al_2O_3 and CeO_2 Surfaces with SO_2 and $SO_2 + O^{2-}$ Studied by X-ray Photoelectron Spectroscopy. *J. Phys. Chem. B* **2005,** *109*, 11712–11719.

(35) Baltrusaitis, J.; Cwiertny, D. M.; Grassian, V. H. Adsorption of Sulfur Dioxide on Hematite and Goethite Particle Surfaces. *Phys. Chem. Chem. Phys.* **2007,** *9*, 5542–5554.

(36) Rodriguez, J. A.; Jirsak, T.; Freitag, A.; Larese, J.; Maiti, A. Interaction of SO_2 with MgO(100) and Cu/MgO(100): Decomposition Reactions and the Formation of SO_3 and SO_4. *J. Phys. Chem. B* **2000,** *104*, 7439–7448.

(37) Chameides, W. L.; Davis, D. D. The Free Radical Chemistry of Cloud Droplets and its Impact Upon the Composition of Rain. *J. Geophys. Res.* **1982,** *87*, 4863–4877.

(38) Rubasinghege, G.; Lentz, R. W.; Park, H.; Scherer, M. M.; Grassian, V. H. Nanorod Dissolution Quenched in the Aggregated State. *Langmuir* **2009,** *26*, 1524–1527.

(39) Rubasinghege, G.; Lentz, R. W.; Scherer, M. M.; Grassian, V. H. Simulated Atmospheric Processing of Iron Oxyhydroxide Minerals at Low pH: Roles of Particle Size and Acid Anion in Iron Dissolution. *Proc. Natl. Acad. Sci. U.S.A.* **2010,** *107*, 6628–6633.

(40) Willey, J. D.; Whitehead, R. F.; Kieber, R. J.; Hardison, D. R. Oxidation of Fe(II) in Rainwater. *Environ. Sci. Technol.* **2005,** *39*, 2579–2585.

(41) Miller, W. L.; King, D. W.; Lin, J.; Kester, D. R. Photochemical Redox Cycling of Iron in Coastal Seawater. *Mar. Chem.* **1995,** *50*, 63–77.

(42) Cwiertny, D. M.; Hunter, G. J.; Pettibone, J. M.; Scherer, M. M.; Grassian, V. H. Surface Chemistry and Dissolution of α-FeOOH Nanorods and Microrods: Environmental Implications of Size-Dependent Interactions with Oxalate. *J. Phys. Chem. C* **2009,** *113*, 2175–2186.

(43) Voelker, B. M.; Morel, F. M. M.; Sulzberger, B. Iron Redox Cycling in Surface Waters: Effects of Humic Substances and Light. *Environ. Sci. Technol.* **1997,** *31*, 1004–1011.

(44) Zhuang, G. S.; Yi, Z.; Duce, R. A.; Brown, P. R. Link Between Iron and Sulfur Cycles Suggested by Detection of Fe(II) in Remote Marine Aerosols. *Nature* **1992,** *355*, 537–539.

(45) Nadtochenko, V. A.; Kiwi, J. Photolysis of $FeOH^{2+}$ and $FeCl^{2+}$ in Aqueous Solution. Photodissociation Kinetics and Quantum Yields. *Inorg. Chem.* **1998,** *37*, 5233–5238.

(46) Lim, M.; Chiang, K.; Amal, R. Photochemical Synthesis of Chlorine Gas from Iron(III) and Chloride Solution. *J. Photochem. Photobiol., A* **2006,** *183*, 126–132.

(47) Hsu, C. L.; Wang, S. L.; Tzou, Y. M. Photocatalytic Reduction of Cr(VI) in the Presence of NO_3^- and Cl^- Electrolytes as Influenced by Fe(III). *Environ. Sci. Technol.* **2007,** *41*, 7907–7914.

(48) Phares, D. J.; Rhoads, K. P.; Johnston, M. V.; Wexler, A. S. Size-Resolved Ultrafine Particle Composition Analysis 2. Houston. *J. Geophys. Res.* **2003,** *108*, 14.

(49) Schneider, T.; Jensen, K. A. Combined Single-Drop and Rotating Drum Dustiness Test of Fine to Nanosize Powders Using a Small Drum. *Ann. Occup. Hyg.* **2008,** *52*, 23–34.

(50) Tsai, C. J.; Wu, C. H.; Leu, M. L.; Chen, S. C.; Huang, C. Y.; Tsai, P. J.; Ko, F. H. Dustiness Test of Nanopowders Using a Standard Rotating Drum with a Modified Sampling Train. *J. Nanopart. Res.* **2009,** *11*, 121–131.

(51) Langridge, J. M.; Gustafsson, R. J.; Griffiths, P. T.; Cox, R. A.; Lambert, R. M.; Jones, R. L. Solar Driven Nitrous Acid Formation on Building Material Surfaces Containing Titanium Dioxide: A Concern for Air Quality in Urban Areas? *Atmos. Environ.* **2009,** *43*, 5128–5131.

(52) Nicolas, M.; Ndour, M.; Ka, O.; D'Anna, B.; George, C. Photochemistry of Atmospheric Dust: Ozone Decomposition on Illuminated Titanium Dioxide. *Environ. Sci. Technol.* **2009,** *43*, 7437–7442.

(53) Sadrnezhaad, S. K.; Ahmadi, E.; Mozammel, M. Kinetics of Silver Dissolution in Nitric Acid from $Ag-Au_{0.04}-Cu_{0.10}$ and $Ag-Cu_{0.23}$ Scraps. *J. Mater. Sci. Technol.* **2006,** *22*, 696–700.

(54) Elzey, S.; Grassian, V. Agglomeration, Isolation and Dissolution of Commercially Manufactured Silver Nanoparticles in Aqueous Environments. *J. Nanopart. Res.* doi: 10.1007/s11051-11009-19783-y.

(55) Ivanova, O. S.; Zamborini, F. P. Size-Dependent Electrochemical Oxidation of Silver Nanoparticles. *J. Am. Chem. Soc.* **2009,** *132*, 70–72.

(56) Chaki, N. K.; Sharma, J.; Mandle, A. B.; Mulla, I. S.; Pasricha, R.; Vijayamohanan, K. Size Dependent Redox Behavior of Monolayer Protected Silver Nanoparticles (2−7 nm) in Aqueous Medium. *Phys. Chem. Chem. Phys.* **2004,** *6*, 1304–1309.

(57) Finlayson-Pitts, B. J. Reactions at Surfaces in the Atmosphere: Integration of Experiments and Theory as Necessary (but not necessarily sufficient) for Predicting the Physical Chemistry of Aerosols. *Phys. Chem. Chem. Phys.* **2009,** *11*, 7760–7779.

(58) Stokes, G. Y.; Chen, E. H.; Buchbinder, A. M.; Paxton, W. F.; Keeley, A.; Geiger, F. M. Atmospheric Heterogeneous Stereochemistry. *J. Am. Chem. Soc.* **2009,** *131*, 13733–13737.